International Journal for Multidisciplinary Research (IJFMR)
E-ISSN: 2582-2160 ● Website: www.ijfmr.com ● Email: editor@ijfmr.com

# Polymerase Chain Reaction Microchip and PID Controller Based Thermal Cycler Design

**Gamze Tilbe İnce[1], Mehmet Yüksekkaya[2], Orhan Erdem Haberal[3]**

[1]Ph.D, Program of Biomedical Equipment Technology, Başkent University, Ankara, Turkey
[2,3]Assistant Professor, Biomedical Engineering Department, Ankara University, Ankara, Turkey

**Abstract**
Numerous specific procedures are needed for nucleic acid detection using traditional approaches. Because of the time and instrumentation requirements, poor detection limits, and other factors, they are behind in creating point-of-care (POC) testing. In addition, some of these traditional approaches can be extremely sensitive. Microfluidic technologies are being used to overcome these challenges by enabling the efficient and automatic performance of all analytical stages, such as sample pre-treatment, reactions, separations, and diagnostics in microchannels on a small chip. The use of microfluidics technology in polymerase chain reaction (PCR) technology has resulted in many advantages. PCR microchips and portable thermal cyclers that can be used for POC testing have enabled faster amplification with accurate results. This paper proposes a low-cost, fast enough thermal cycler for POC testing that uses a polymer-glass microchip and an affordable Peltier element to quickly heat samples. A laser cutter was used to build the microchip needed to perform PCR, which was designed using a computer-aided design (CAD) software. The heating and cooling elements employed in the creation of the thermal cycler were Peltier elements, heat sink, centrifugal fan, and CPU fan. A microcontroller and H-Bridge modules were used to control the temperature with the help of proportional-integral-derivative (PID) controller algorithm. After that, the circuit components and PID control algorithm—which was created for temperature control—were combined to create the PCR cycle. The analysis focuses on the heating and cooling performances of suggested thermal cycler.

**Keywords:** Polymerase Chain Reaction, PID Control, Microchip, Thermal Cycler, Point of Care Testing

## 1. Introduction

Kary B. Mullis developed the Polymerase Chain Reaction (PCR) technique in 1985, which made it possible for scientists to replicate rare DNA samples millions of times. The PCR is a three-step procedure that happens at various constant temperatures. The steps are annealing (at 55–60 °C), denaturation (at 90–95 °C), and extension (at 70–72 °C). The double helix of the DNA separates into two strands when the test tube is heated at denaturation step. As a result, each helix's DNA sequence is revealed, and when the temperature drops, the primers automatically attach to the complimentary regions of the DNA sample at annealing step. The enzyme concurrently forms the proper sequence connections between the free nucleotides and the primer as well as each of the split DNA strands. After completing the reaction, two double helices with the desired part of the original are produced at elongation or extension step. A single copy of a DNA molecule can multiply to hundreds of millions of copies after thirty to forty cycles. Many aspects of modern study have been transformed by this

technology, such as the identification of the viruses in human cells and the diagnosis of genetic abnormalities. Because fossils with small amounts of DNA can be used to create enormous quantities of DNA, PCR has an impact on evolutionary studies as well. In 1988, the Taq DNA polymerase was commercially commercialized for widespread use by Kary Mullis and Cetus Corporation. Since the invention of the first PCR cyclers, automated technologies have replaced water baths as the primary method of amplifying DNA. Despite tremendous advancements in the field, DNA amplification is challenging due to Taq DNA polymerase's instability at high temperatures. Several hot start-based techniques were created in the 1980s to address Taq DNA polymerase's poor sensitivity and inefficiency at high temperatures. According to researchers, PCR will remain significant in biomedical research and human health in the long run, even with the advent of next generation polymerases and real-time and digital PCR technology [1]–[6].

Since the first PCR device based on microfluidic technology was introduced, numerous methods have been developed. These microfluidics-based PCR devices are designed to reduce costs associated with manufacturing and handling, increase efficiency, decrease instrument complexity, shorten the time needed for DNA amplification, use less biological sample than is necessary for PCR, produce fewer non-specific products, and be portable and integrated. Although microfluidic-based devices provide substantial benefits compared to traditional benchtop devices, many PCR users have limited opportunities to utilize microfluidic methods [7]–[10].

Using micro-electromechanical systems technology, glass or silicon are used to create the first generation of microfluidic chips. Typically requiring specialist equipment, this procedure is unsuitable for large-scale production. Microchips for DNA extraction, PCR amplification, and DNA fragment separation have been fabricated on a range of substrates, including non-traditional polymer-based materials like silicon and glass. Glass, silicone, quartz, ceramics, and polymers like polymethylmethacrylate (PMMA), cyclic olefin copolymer (TOPAS), polystyrene (PS), polycarbonate (PC), and polydimethylsiloxane (PDMS) are a few examples of materials that are often used in manufacturing [11], [12].The selection of microchip materials is based on their good optical performance, interchangeable characteristics, good electrical insulation and heat dissipation, good biocompatibility, and not having a reaction with the operating environment and, inexpensive and easy to produce [13], [14].

There are two types of chip-based micro-PCR devices: continuous flow PCR chips and well/chamber-based PCR chips. There are two types of chip-based micro-PCR devices: continuous flow PCR chips and well/chamber-based PCR chips. Chamber-based PCR chips come in three basic shapes: single-chamber, droplet virtual chamber, and array-chamber. They are miniature replicas of conventional thermal cyclers. The PCR mixture is fed into the chamber during chamber-based PCR, after which the entire chip—including the amplified sample—is heated to and cooled to predetermined thermal cycling temperatures. Large total thermal mass in chamber-based PCR instruments might lead to unfavorable thermal inertia and longer thermal cycle times. Continuous-flow micro-PCR is one of the more popular forms of micro-PCR because it may be integrated with a variety of functional units. To accomplish the necessary temperature cycling, continuous flow micro-PCR continually transfers the sample across zones of constant temperature. Because only the PCR mixture is heated and cooled - rather than the entire chip - the continuous flow micro-PCR technique has a lower thermal inertia. This enables quick thermal cycling while using less energy, which qualifies the technology for inclusion into µ-TAS and portable applications. However, because PCR components have high surface adsorption because of the

large surface/volume ratio times, PCR inhibition has shown to be a significant difficulty for continuous flow micro PCR [15]–[18].

### 1.2. PID Controller and Tuning Methods

Subsystems and processes that cooperate to produce an output with the desired performance given a specific input make up control systems. The goal of control systems is to use its component parts to manipulate the outputs in accordance with a given set of inputs. The selection of control systems is based on three factors: power amplification, remote control, and disturbance correction [19]. The Proportional Integral Derivative (PID) Controller is a general control loop feedback mechanism widely used in industrial control systems. The PID controller calculates the "error" value, which is the difference between the measured system variable and a fixed set point. The system uses the controller to minimize the error by adjusting the control inputs [20].

The basic PID controller can be written mathematically, a control signal is the sum of three mathematical operations:

$$u(t) = Kp.e(t) + Ki\int_0^t e(\tau)d\tau + Kd.\frac{de}{dt}, \qquad (1)$$

In this equation u is the control signal, Kp is the proportional gain, Ki is the integral gain, Kd is the derivative gain (Kp, Ki, Kd are tuning parameters), e is the error, t is time or instantaneous time. Each term is preceded by a constant (Kp, Ki, Kd). These are known as tuning constants. When properly selected, they enable the controller to provide a control signal that will reduce the error to zero. Improper tuning of Kp, Ki and Kd can lead to overshoot, long processing time, instability, and oscillations [21], [22].

The proportional (P) controller modifies the output in proportion to the current error value. The proportional response can be changed by multiplying the error by a constant value "Kp," which is known as proportional gain. The advantage of P Control is that it is easy to implement and can take the process close to the desired setpoint. However, the error never automatically goes to zero, so the process never reaches the setpoint. It also cannot automatically eliminate offset and steady state error [22], [23].

The effect of the integral controller (I) is proportional to both the magnitude of the error and the duration of the error. Summing the instantaneous error over time (the integral of the error) gives the accumulated offset that must be corrected earlier. The accumulated error is then multiplied by the integral gain and added to the controller output. The magnitude of the contribution of the integral term to the total control action is determined by the integral gain "Ki.". The main advantage of the integral controller (I) is that it allows to eliminate the steady state error. By adjusting the Ki term, the control performance of the integral controller can be tuned [23], [24].

Since the integral controller does not have the ability to predict the future behavior of the error, it reacts normally when the set point changes. The derivative controller (D) solves this problem because it can predict the future behavior of the error. The rate of change of the system error is calculated by determining the slope of the error over time and multiplying this rate of change by the derivative gain "Kd". The magnitude of the contribution of the derivative term to the control action is called the derivative gain (Kd) [23], [25]. As a result, the PID controller's job is to take the error signal and perform three separate mathematical operations on it (Figure 1).

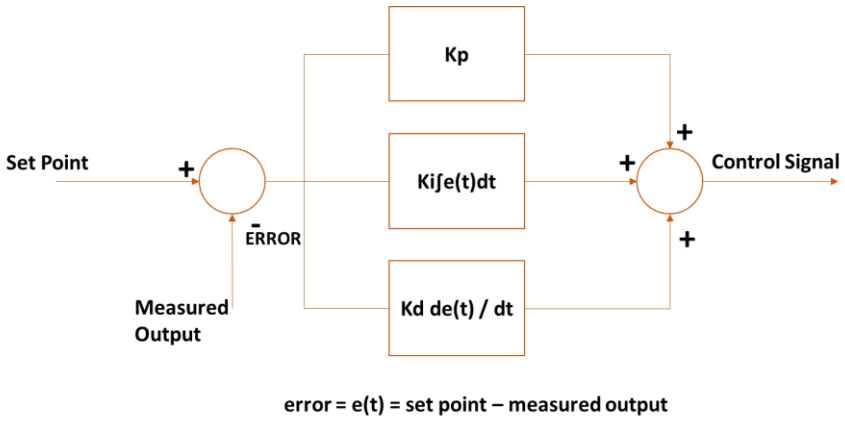


**Figure 1: PID Control System Block Diagram**

Several PID tuning methods are suggested in the literature. Some of these are [23], [26], [27]; Ziegler–Nichols Method, Chien – Hrones – Reswick Method, Cohen–Coon Method, Refined Ziegler–Nichols Method, Wang – Juang – Chan Method, Optimum Method, Trial & Error Method and, Auto Tuning Method. One of the simplest methods for determining the value of the PID parameter is trial and error method. There is no need for mathematical operations with this method. It is necessary to set the values of Ki and Kd to zero before raising the Kp. The advantages of this method are it is a quick and simple method to get an acceptable outcome, process knowledge is not very necessary, and it requires an intuitive approach. Besides these getting a good performance is a long process and reaching a solid and stable solution is not guaranteed in this method [27], [28].

The following qualities affect a closed-loop system's performance:

- Rise time: The time it takes for the system output to rise above 90% of the desired level for the first time.
- Overshoot: How much higher the peak level is relative to the steady state is normalized to the steady state.
- Settling Time: The time it takes for the system to approach its steady state.
- Steady State Error: The difference between the steady state output and the desired output.

The individual effects of three parameters (Kp, Ki, Kd) on the performance of the system are summarized in Table 1. Kp, Ki and Kd must be adjusted together to achieve the desired performance. According to Table 1, for example, when Kp and Ki are constant, increasing Kd alone creates a small change in the rise time, reduces overshoot and settling time, and is ineffective on the steady-state error. At the same time, while Ki and Kd are constant, increasing Kp alone reduces the rise time, increases the overshoot, slightly increases the settling time, and reduces the steady-state error.

**Table 1: Effect of PID Parameters on the System**

| Parameters | Rise Time | Overshoot | Settling Time | Steady State Error |
|---|---|---|---|---|
| **Kp** | Decreases | Increases | Small Increase | Decreases |
| **Ki** | Decreases | Increases | Increases | Eliminate |
| **Kd** | Small Change | Decreases | Decreases | No effect |

### 1.2. Temperature Control in Thermal Cyclers

Temperature control is one of the most significant variables in a thermal cycler device. The temperature

of the PCR tube containing the DNA sample must be changed rapidly, precisely, and repeatedly during the process of thermal cycling for the PCR to be successful and efficient. In most commercial thermal cyclers available on the market, temperature control is usually achieved by PID control due to its simple algorithm, robustness, and stability. The purpose of the PID temperature controller is to heat the PCR block to the correct temperature and then maintain it at that temperature. The performance of the temperature controller depends on the values of the Kp, Ki, and Kd of the PID controller. Setting an inappropriate gain value in the controller causes the desired temperature to be exceeded or below. Delays are introduced by under- or overshooting the temperature set points, and overheating may cause harm to the DNA sample. In contrast, undershooting can result in incomplete reactions since the DNA mixture does not reach the desired temperature for a sufficient amount of time [21], [29].

Thermal cyclers designed using different PID controllers are given in the Table 2. A study successfully amplified lambda phage gene by using PID temperature controller [30]. This study differs from other studies as a continuous flow PCR. It has not been shown whether amplification was successful in some of other thermal cyclers, however many of them have been successful in reaching PCR step temperatures. Another study found that the fuzzy-PID algorithm may correct the classic PID's significant overshoot problem while simultaneously reducing the adjustment time [31]. In a study researchers said that using the transfer function model, the PID controller has the lowest maximum peak overshoot, settling time, delay time, and rise time when compared to the other controllers [20]. A fuzzy-PID algorithm-based system can precisely control the temperature to within ± 0.2°C. Besides, it is said that the improved PID control algorithm can eliminate the overshoot situation. Accurate PCR findings were obtained by combining fuzzy-PID algorithm with the circuit elements utilized [32]. Although the control methods used in the studies are similar, the designs differ in terms of circuit elements. Also in most of the studies, the tuning method was not mentioned.

**Table 2: Comparison of Thermal Cycler Devices Controller Type and PCR Conditions**

| Reference | Controller Type | PCR Conditions | Amplification |
|---|---|---|---|
| [30] | PID | Denaturation: 93.42°C ± 0.21 Annealing: 56.35°C ± 0.30 Extension: 73.20°C ± 0.31 | lambda phage gene |
| [31] | fuzzy-PID | Denaturation: 95°C Annealing: 60°C Extension: 72°C | - |
| [20] | PID | Denaturation: 94°C Annealing: 55°C Extension: 72°C | - |
| [32] | fuzzy-PID | Denaturation: 98°C Annealing: 55°C Extension: 72°C | β-actin gene |
| [33] | Optimized PID | Denaturation: 95°C Annealing/Extension: 65°C | DNA segments of SEC61 translocon subunit alpha, Matrix Met- |

| | | | |
|---|---|---|---|
| | | | al- lopeptidase, and ORF1ab |
| [34], [29] | PI | Denaturation: 94°C Annealing: 50°C; Extension: 72°C | six DNA samples |
| [35] | PID | Denaturation: 95°C Annealing/Extension: 60°C | T. pallidum (Syphilis) bacterial DNA and Zika virus RNA samples |
| [36] | hybrid fuzzy PID | Denaturation: 95°C Annealing/Extension: 70°C | - |

## 2. Materials and Methods

A PCR thermal cycler with Peltier elements and a CPU fan was designed. A chamber-based PCR microchip was produced using a double-sided adhesive (DSA), a glass substrate and polymethylmethacrylate (PMMA). The Peltier element was placed under the chamber for heating process. The CPU fan and a centrifugal fan were used for cooling process. The temperature control of the device was provided by the PID controller. In this study, a 12V power supply and as a microcontroller Arduino nano was used.

### 2.1. Micro PCR Chip Design

PMMA, DSA and glass slide were used for microchip fabrication, and a three-layer design was conducted using laser cutter. When selecting the DSA, 3M™ products were reviewed. DSA were selected to be chemically inert and have high temperature resistance, and thicknesses not exceeding ~1mm. 3M™ 9965 was chosen and used because it was developed specifically for use in microfluidic applications or medical device designs. 24 mm x 50 mm, 24 mm x 32 mm, and 22 mm x 22 mm sized glass slides with a thickness between 0.13 and 0.17 mm were provided.

Different sizes of microchip designs have been made. The microchip sizes were determined as 24 mm x 50 mm, 24 mm x 32 mm, and 22 mm x 22 mm. When designing the microchip channel, the channel volume of 10 µL and above was taken into consideration and necessary calculations were made. The microchannel width was kept constant (4 mm or 5mm). The volume was calculated by varying the channel length and depth. For example, when the channel width was 5 mm, length 19 mm and depth 0.18 mm or more, the volume was greater than 10 µL and the desired volume was obtained for 24 mm x 32 mm sized PCR microchip. After determining the channel width, length and depth, the microchip design was realized using a computer-aided three-dimensional (3D) design program. Figure 2 shows 22 mm x 22 mm PCR microchip design. The diameter of the sample inlet and outlet holes was determined as 0.70 mm, and the microchip alignment holes were selected with a diameter of 2 mm, for DSA and PMMA layers. After the 3D design was determined, DSA and PMMA were cut according to the design using a laser cutter (Figure 3).

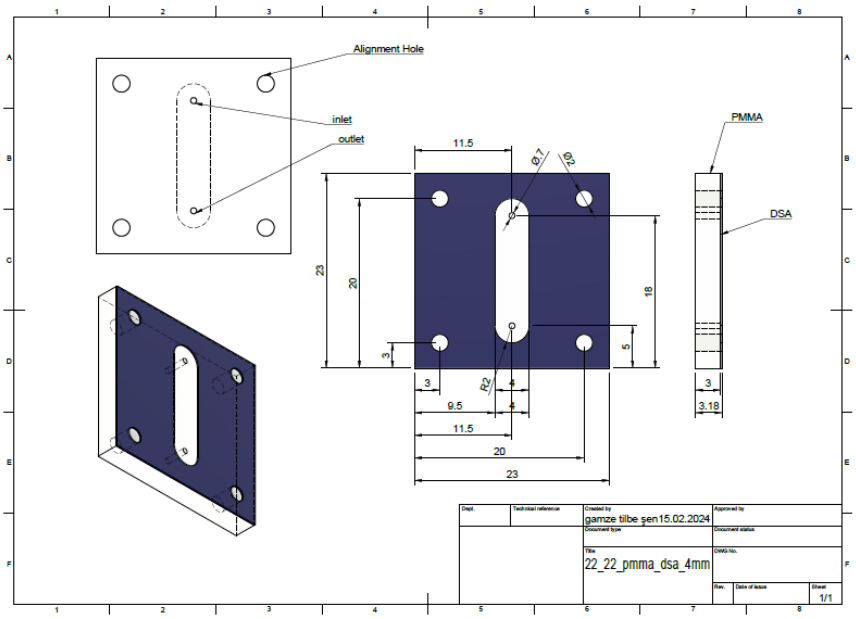


**Figure 2: 22 mm x 22 mm microchip design has a volume of 10 µL**


**Figure 3: The fabricated PCR microchip (24 mm x 50 mm). Layers of DSA and PMMA cut with a laser cutter and combined (The channel of the combined PCR chip is filled with ink)**

### 2.2. Thermal Cycler Circuit Design

The thermal cycler design consists of heater-cooler elements (Peltier element, fan), temperature sensor for temperature measurement and a control circuit (microcontroller, H-bridge, relay) (Figure 4).

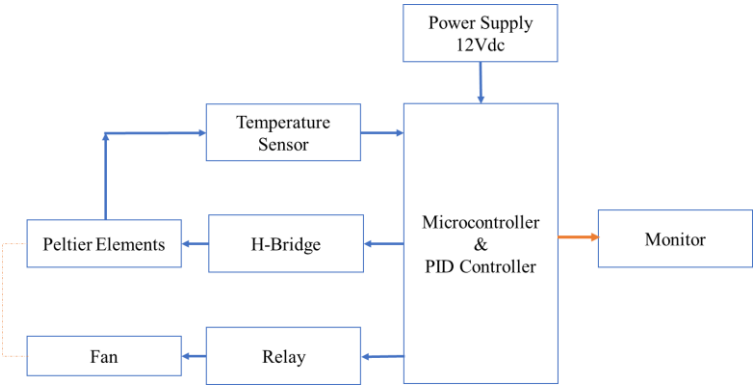


**Figure 4: Temperature Control of Peltier Element with PID Controller**

**Peltier Elements:**

An entirely solid-state heat pump, a thermoelectric device works on the principle of the Peltier effect, which states that heat is transferred from a hot to a cool junction by electrons carrying energy. Thermoelectric devices can function as efficient sources of heating and cooling if they are designed properly [37]. Peltier elements were used to perform heating-cooling processes. Peltier elements were evaluated in terms of size, operating temperature, maximum current, maximum voltage, and prices. It is necessary to ensure full contact of the microchip with the Peltier element and ensure transmission between the Peltier element and the microchannel without losing heat. Therefore, Peltier sizes and thickness are important. Two Peltier elements were selected to be studied (Table 2). Peltier elements selected to be used in the application are manufactured by Laird Thermal Systems and Marlow Industries.

**Table 2: Peltier elements specifications table**

| Peltier Product Number | Operating Temperature | Current - Max | Voltage - Max | Length X Width | Height |
|---|---|---|---|---|---|
| **PCX7.5,13,F1,4023,TA,RT,W6** | 120°C | 7.7A | 15.3V | 40.00mm L x 23.00mm W | 2.80mm |
| **RC12-8-01LS** | 130°C | 7.4A | 14.7V | 44.70mm L x 40.13mm W | 3.53mm |

**Temperature Sensor:**

DS18B20 temperature detector sensor was provided. The temperature detection range is -55℃ and +125℃. In the range of -10℃~+85℃, its accuracy is ±0.5. This sensor can be controlled with a single microcontroller pin because the DS18B20 operates according to the 1-wire standard. DS18B20 has 3 pins in total, which are $V_{cc}$ (5V), ground and data pin.

**Microcontroller:**

Arduino Nano board was used as the microcontroller. The Nano is the smallest board made by Arduino, measuring 45 mm in length and 18 mm in width. It weighs only 7 grams. Arduino Nano is a microcontroller board based on ATmega328. It has 20 digital input/output pins, 8 analog inputs, 6 PWM inputs, a 16 MHz ceramic resonator, a mini-USB port. The card can operate with an external source of 6 to 20 volts. ATmega328 has 32 KB of memory. It also includes 2 KB SRAM and 1 KB EEPROM. Arduino Nano can be programmed with Arduino Software (IDE), Arduino CLI and Web Editor. We used Arduino IDE to program Nano board in this work.

**Fan:**

To achieve rapid cooling, a liquid-cooled fan is used, and cooling efficiency is increased. To achieve this, Rampage Helios C1 Series Liquid Cooling System was preferred. Thermal compound copper plate of this fan ensures that it is an element with more efficient heat transfer and better thermal conductivity. The pump unit does not take up much space and can provide high-speed circulation. In addition to the liquid-cooled fan, a centrifugal fan was preferred to be used to ventilate a specific desired point or area. A centrifugal fan is a motor or pump that pushes air by moving it inside and pushing it out at a 90-degree angle. While the fan is an electrical device that moves the air, the centrifugal fan is a mechanical device consisting of a fan, directing the air from the fan, and sending it to a certain point.

**H-Bridges:**

In this study, thermal cycler performance was evaluated using different H-bridges. The H-bridges whose performances were assessed are L298N, TB6612FNG and BTS7960. After evaluating the performances, BTS7960 H-bridge was selected for study. BTS7960 is an integrated high current half bridge for motor drive applications. A single IC contains a p-channel high-side MOSFET and an n-channel low-side

MOSFET. Because of the P-channel high side switch, the need for a charge pump is eliminated. Integrated driver circuitry with logic level inputs, current sensing diagnostics, slew rate adjustment, inactive time generation, and protection against overtemperature, overvoltage, undervoltage, overcurrent, and short circuit makes it easy to interface to a microcontroller. Additionally, the BTS7960 provides a cost-optimized solution for high-current PWM motor drivers. This module allows controlling DC motors using the PWM (Pulse Width Modulation) technique. Additionally, it converts a constant input voltage into a variable voltage for the motor. Speed can be controlled by changing the DC motor voltage.

**Relay:**

Relays are one of the basic components used in the electronics industry. A relay is defined as an electromagnet that acts as a switch by opening and closing electrical contacts to control current. Relay modules can provide usage areas from single channel to double channel, from four channels to eight channels, depending on the need. A single-channel relay can only control one circuit at a time since it only has one switch or channel. Usually, this kind of relay is employed in basic applications where just one load needs to be switched. In this work a single channel relay was used to control CPU and centrifugal fan for cooling process.

**Bluetooth Module:**

HC-06 Bluetooth Module is a wireless communication module that provides wireless communication and uses the Bluetooth protocol for wireless communication. This module supports Bluetooth 2.0 and provides communication distance of up to 10 meters by communicating at 2.4 GHz frequency. In this work, the HC-06 Bluetooth module was used to display temperatures through an Android device.

After the electronic materials are provided, PCB design has been made to make the temperature control circuit portable, reliable, and less complex (Figure 5).

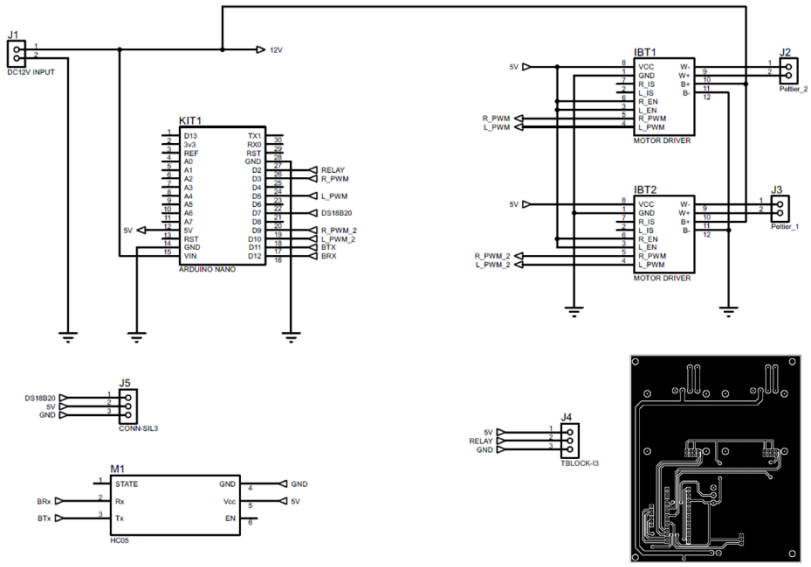


**Figure 5: PCB Design with components H-Bridge, Temperature sensor, Bluetooth Module, Relay, and Arduino Nano**

### 2.3. Micro Thermal Cycler Box Design

While designing the thermal cycler box, a CPU fan was used in contact with the Peltier surface to cool the Peltier element. The CPU fan to be used must contact the cold surface. If not, the Peltier will exceed

a certain temperature and cause disruptions in the PCR cycle. To prevent such a negative situation from occurring, a circuit and system has been designed to ensure that the Peltier element and fan operate under ideal conditions. Box size is designed as 300 mm x 300 mm x 150 mm (Figure 6).

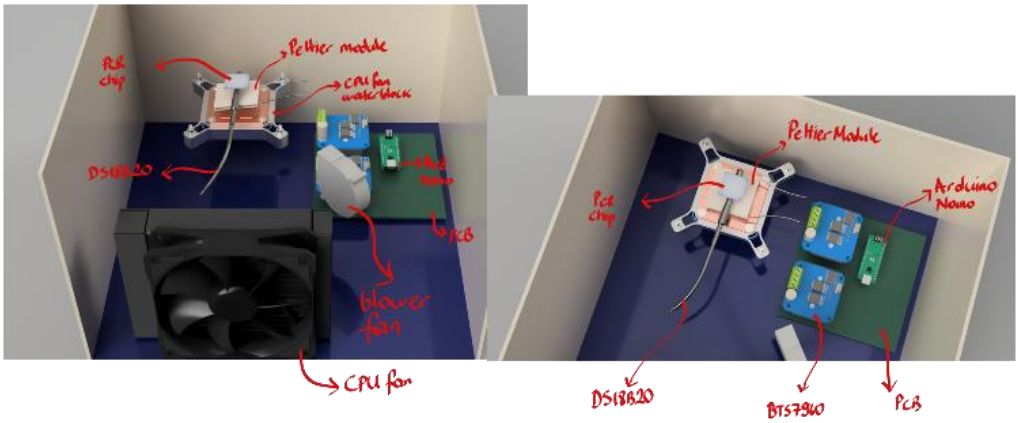


**Figure 6: Thermal Cycler Box Design**

In the box design, the section where the PCR chip will be located is designed as a separate section within the box and with a cover. The part with a cover makes it simple to access the disposable PCR chip, which may be placed inside and taken out after the procedure is over Additionally, it is simpler to get the required temperatures because of the small volume. With the addition of a Bluetooth module to the design, an Android device will be able to monitor temperature changes associated with the PCR cycle, the number of cycles, and both the start and end of the process.

## 3. Experimental

Using the TB6612FNG H-Bridge, for a complete PCR cycle, the power supply is adjusted to 10V and 2.5A for the first measured temperature data (green) and 12V - 3A for the second measured temperature data (red) (Figure 7). PID control parameters Kp, Kd and Ki were 10, 0.05 and 0.05 respectively. However, the TB6612FNG H-Bridge was unable to achieve the required efficiency.

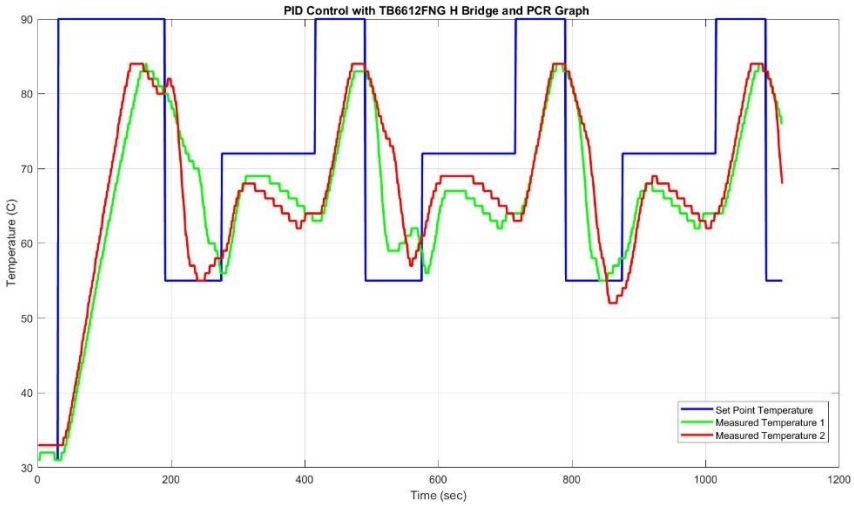


**Figure 7: PCR cycle graph with TB6612FNG H-Bridge (with different currents and voltages; 10V and 2.5A green, 12V - 3A red)**

Two outputs of the L298N H-Bridge module were connected in parallel to repeat the temperature tests on the Peltier elements. The graph in Figure 8 was obtained with the PID controller parameters set as Kp = 5; Ki = 0.017; Kd = 0.5 when the power supply was 10V and 1.5A. It was observed that there were significant differences between the set point and measured temperatures.

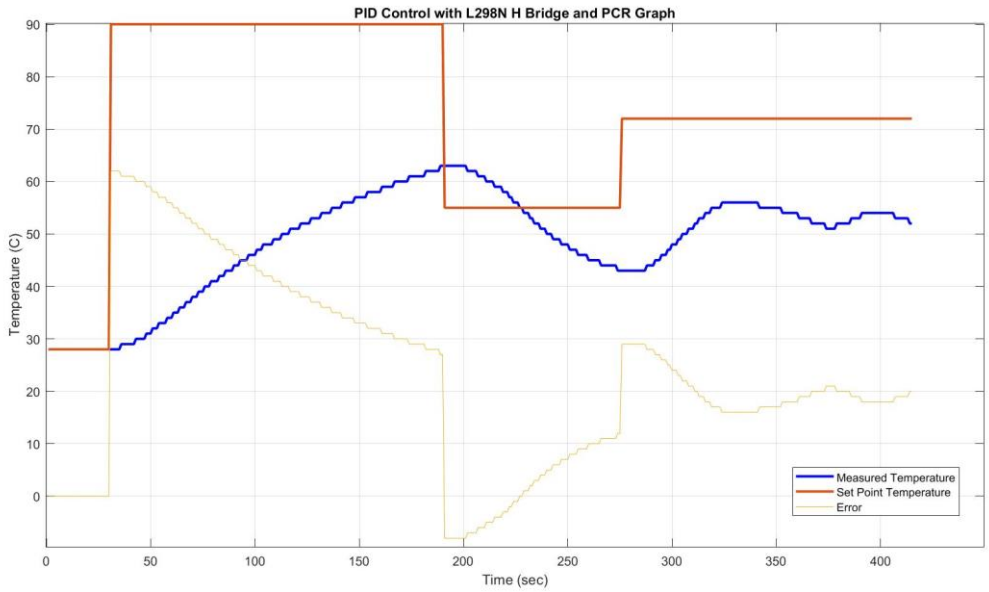


**Figure 8: PCR cycle graph with L298N H-Bridge**

Using the BTS7960 20A H-Bridge module, the circuit shown in Figure 9 was created, the necessary connections for the temperature sensor were made, and the temperatures reached by the Peltier element were measured.

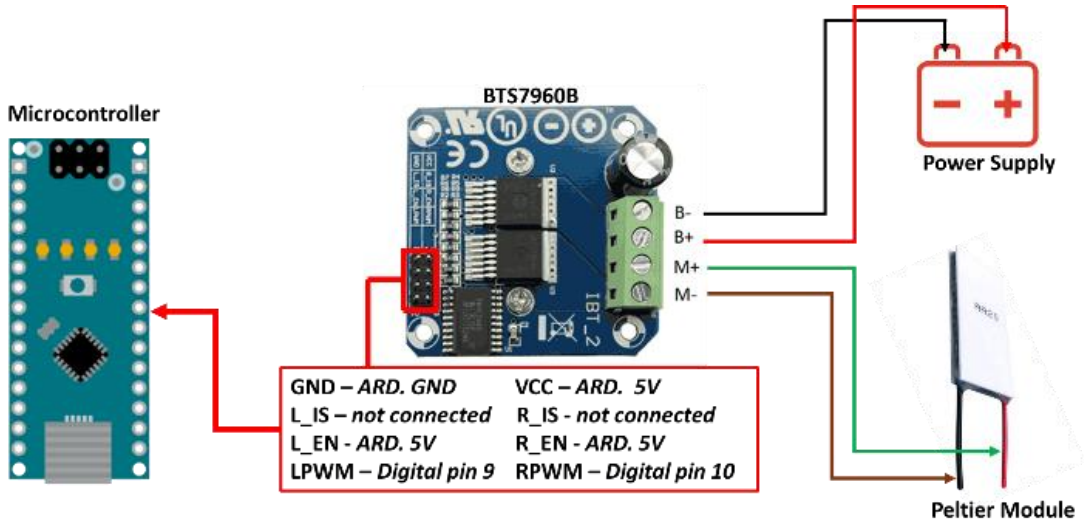


**Figure 9: Circuit diagram created for temperature control with BTS7960B H-Bridge module**

Firstly, it was studied how long it would take Peltier elements to reach 72°C and 55°C, which are the extension temperatures to be used in PCR cycle. The power supply is set to 12V – 5A. PID controller parameters were found using MATLAB – PID Tuner Toolbox. Temperature measurements were carried

out using these parameters. It was observed that the Peltier element reached 72°C in ~45 seconds and 55°C in 20 seconds, and the overshoots were between +3°C and -3°C (Figure 10, Figure 11, Figure 12). The step response of the system (72°C) was obtained using MATLAB – System Identification Toolbox with an experimentally produced transfer function (Figure 11).

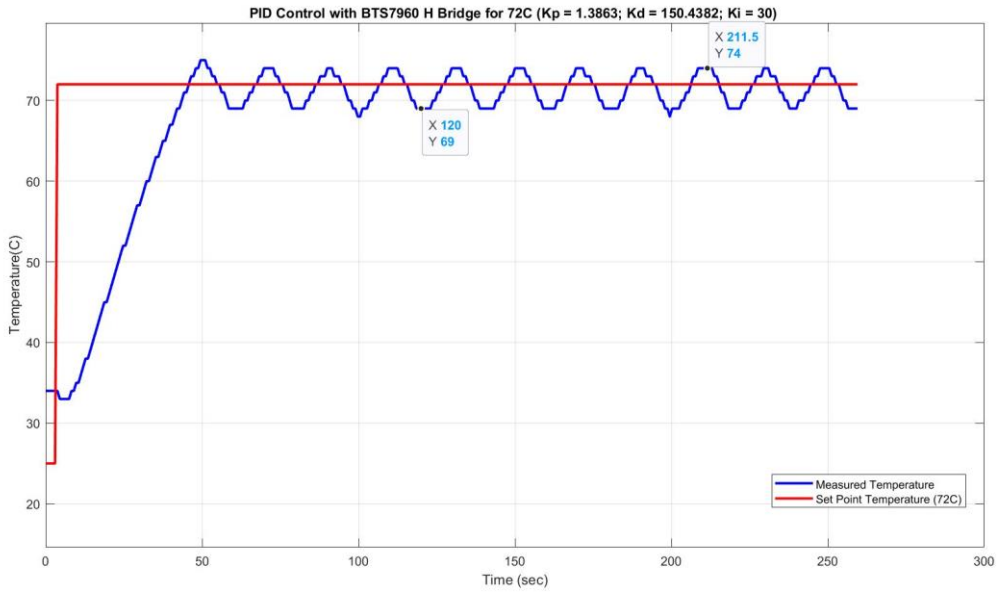


**Figure 10: Extension temperature control with PID controller and BTS7960 H-Bridge.**

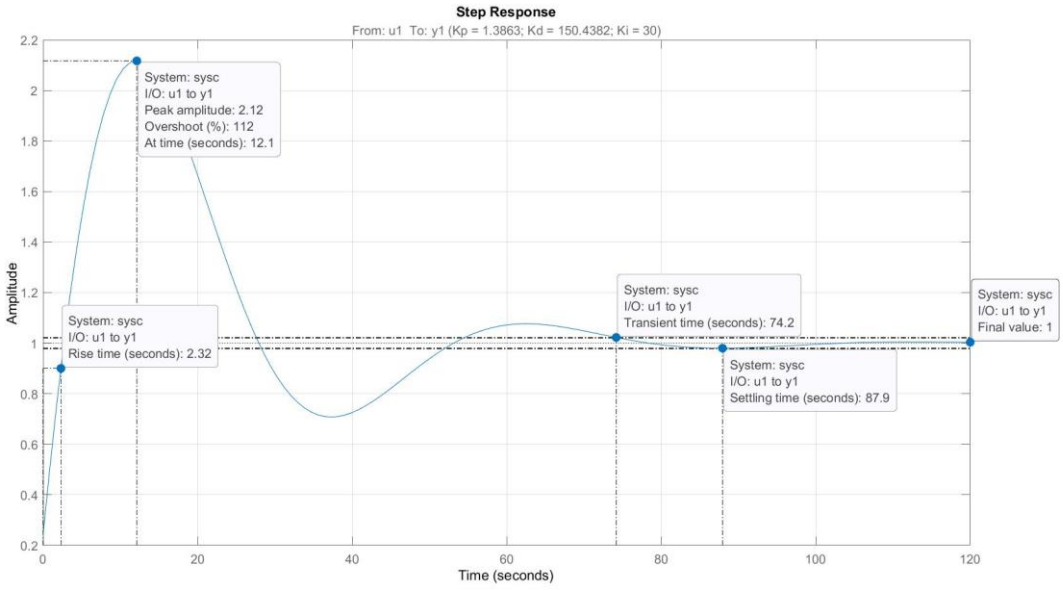


**Figure 11: Step Response of the system (72°C and PID parameters are Kp 1.3863, Ki 30, Kd 150).**

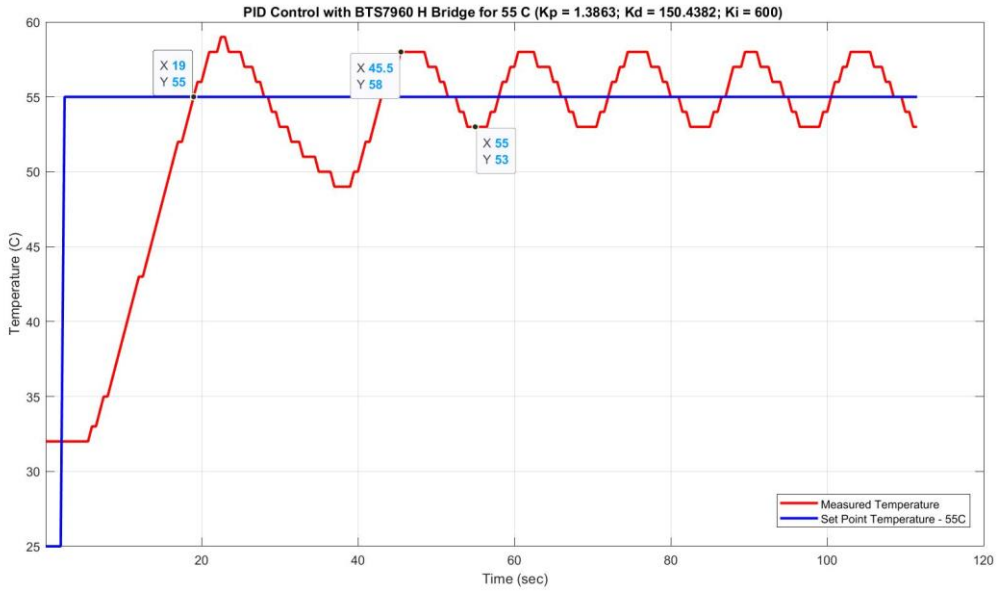


**Figure 12: Annealing temperature control with PID controller and BTS7960 H-Bridge.**

We then studied how long it would take to reach the denaturation temperature (95°C). In this measurement, a Peltier element and a cartridge heater were used as heating elements, but the cartridge heater was found to have a late response time. PID controller parameters were found using MATLAB – PID Tuner Toolbox. Temperature measurements were carried out using these parameters. An experimentally produced process transfer function was used as the basis for determining the PID controller system responses. It was observed that the Peltier element reached 95°C in ~200 seconds, and the overshoots were between +0°C and -3°C (Figure 13).

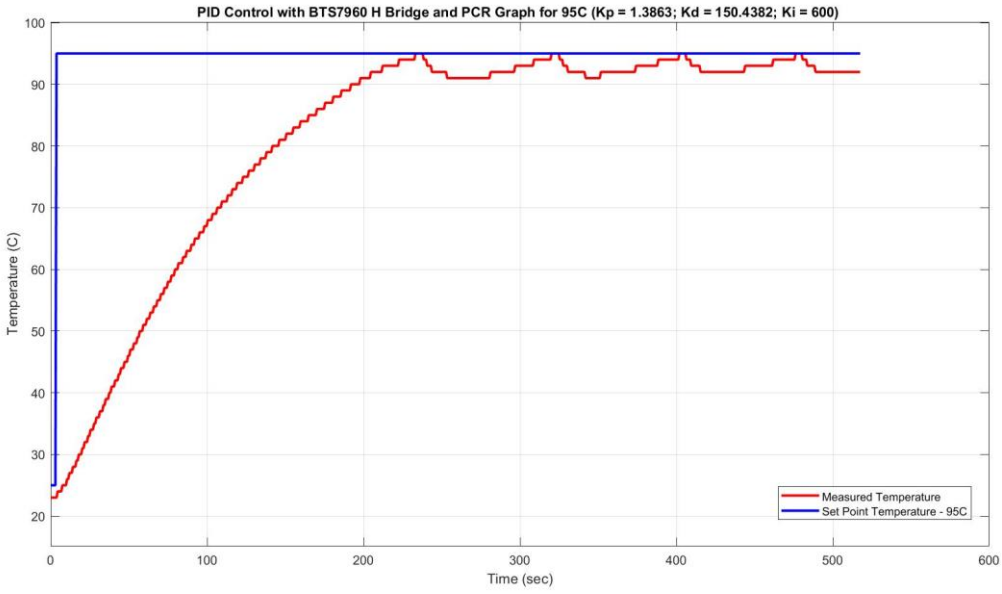


**Figure 13: Denaturation temperature control with PID controller and BTS7960 H-Bridge using a Peltier element and a cartridge heater.**

Figure 14 shows the PCR cycle obtained using 2 BTS7960B H-Bridges. Temperature control was achieved by connecting 2 Peltier elements to 2 separate H-bridges instead of a single H-bridge. 12V – 3A power supply was used when making measurements. PID controller parameters were set as Kp 100, Ki 35, Kd 150, respectively. CPU fan and centrifugal fan control is provided through the relay module. As can be seen from the Figure 14, the desired efficiency was achieved when the BTS7960 H-bridge was used.

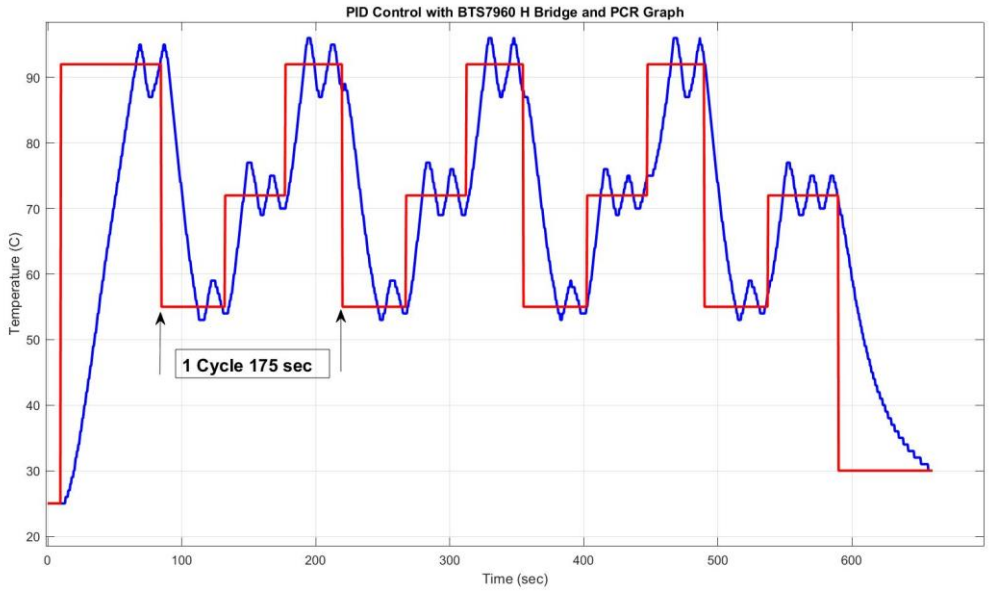


**Figure 14: PCR cycle graph created by controlling 2 Peltier elements via BTS7960 H-bridges.**

## 4. Results

Electronic components employed in this study included relay modules, Peltier elements, H-bridges, Bluetooth module and microcontrollers. PID controller is used to provide precise temperature control. Centrifugal and liquid-cooled fans were used alongside Peltier elements to aid cooling. In addition, a heat sink has been used to provide better cooling of the Peltier elements. Thermal cycler conditions consist of four different temperatures: initial denaturation, denaturation, annealing, extension. There is also a 60 second resting period at the end of the cycle. The denaturation temperature was set at 90°C, annealing temperature at 55°C, extension temperature at 70°C, and resting temperature at 30°C for the first experiments. Denaturation time was determined as 55 sec, annealing time was 60 sec, and extension time was 60 sec. It was seen on the PCR graphs that one cycle lasted 175 seconds. The PCR process, which consisted of a total of 5 cycles lasted 19 minutes and 26 seconds (Figure 15). PID parameters are the same for each graph and Kp, Ki and Kd are 100, 35 and 150, respectively. These parameters were obtained by trial-and-error method. While calculating the PID control parameters by trial-and-error method, the Kp value was first set as 100. Ki and Kd are set to zero. When a regular oscillation was obtained, the Ki value was set to 35 after several different trials. Finally, the Kd value was determined. The different graphs obtained are given below.

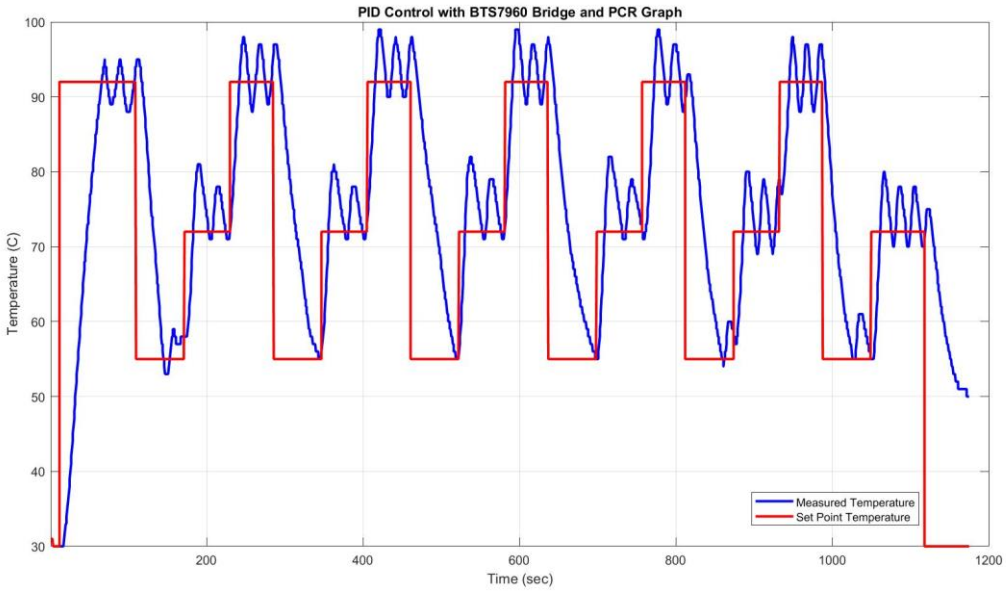


**Figure 15:** PCR graph consisting of 5 cycles with initial denaturation at 92°C for 97 seconds, annealing at 55°C for 60 seconds, Extension at 72°C for 60 seconds, Denaturation at 92°C for 55 seconds.

When the same experiment was repeated without using a CPU fan in the cooling process, the following graph was obtained. This graph illustrates how much more of an impact the CPU fan has on cooling. When using only a centrifugal fan, the annealing temperature of 55°C was never reached (Figure 16).

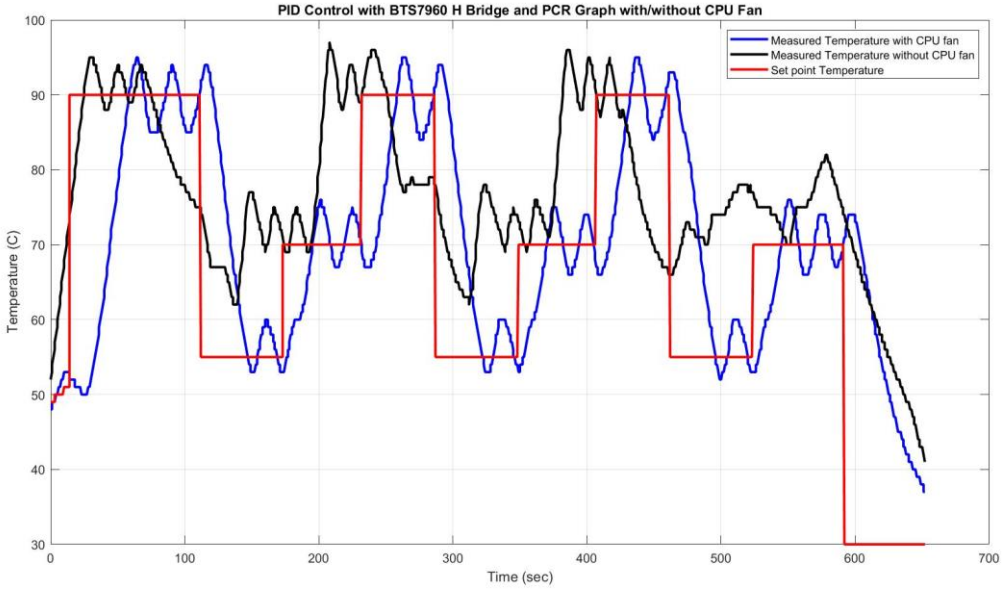


**Figure 16:** PCR Cycle without using a CPU fan.

Then, PCR graphs were created with a cycle time of 180 seconds. In the Figure 17, the PCR cycle consists of initial denaturation (92ºC – 80 sec), annealing (55ºC – 60 sec), extension (72ºC – 60 sec), denaturation (92ºC – 60 sec) and final extension step (72ºC – 5 min). PID parameters were first found by

trial-and-error method and measurements were taken. PID parameters were created using MATLAB – PID Tuner Toolbox and System Identification Toolbox used for transfer function identification, and measurements were taken again under same conditions for the same PCR process. The total process of 5 cycles took ~20 minutes to complete. The results for different PID parameters are given comparatively in the Table 3. According to the Table 3, there were differences in overshoots and rise time. The PID parameters that obtained with trial-and-error method showed a lower rise time but less overshoot. The PID parameters that obtained with PID Tuner Toolbox had +4°C overshoots. This is because of the Kd parameter being zero which determined by the toolbox. The rise time of this system was faster because Kp and Ki were smaller than the first system's Kp and Ki parameters. As can be understood from these results, stable and fast responding systems can be obtained by changing the PID controller parameters.

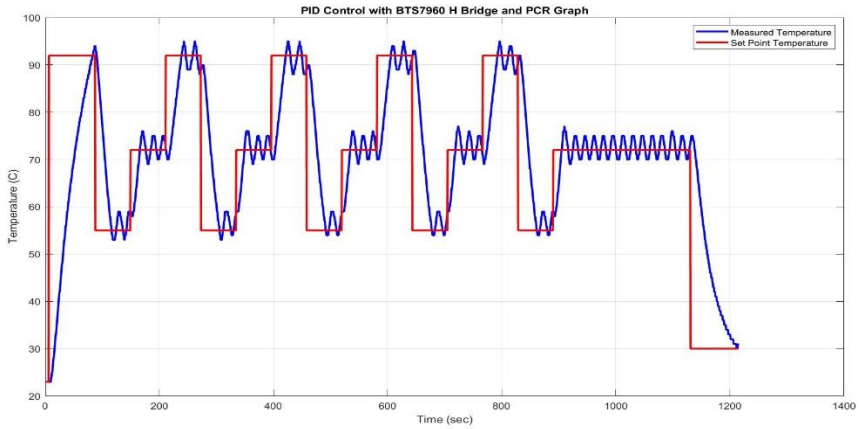


**Figure 17: PCR graph consisting of 4 cycles with initial denaturation at 92°C for 80 seconds, annealing at 55°C for 60 seconds, Extension at 72°C for 60 seconds, Denaturation at 92°C for 60 seconds and and final extension step at 72ºC for min. PID parameters are determined by Trial & Error method (Kp=100, Ki=35, Kd=150).**

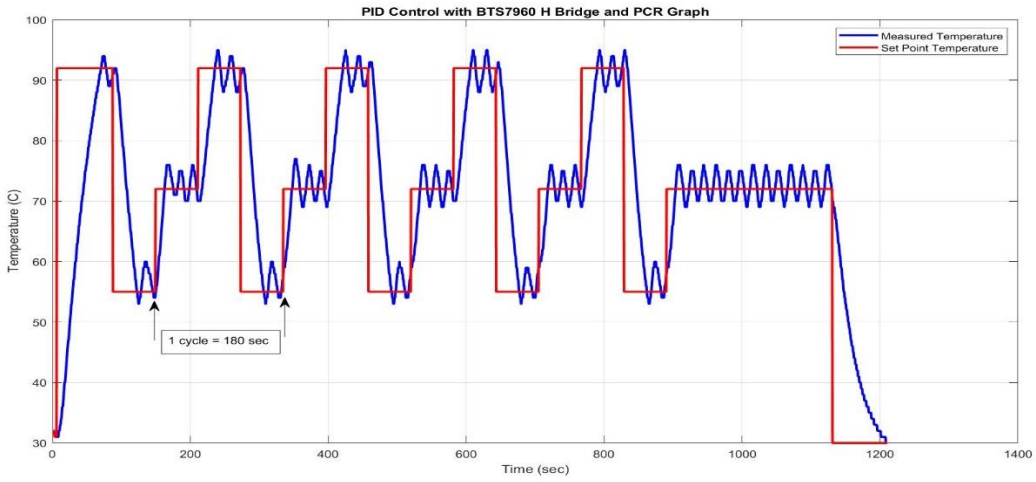


Figure 18: PCR graph consisting of 4 cycles with initial denaturation at 92°C for 80 seconds, annealing at 55°C for 60 seconds, Extension at 72°C for 60 seconds, Denaturation at 92°C for 60 seconds and final extension step at 72ºC for min. PID parameters are determined by MATLAB-PID Tuner Toolbox (Kp=1.4602, Ki=3.1074, Kd=0).

**Table 3: Comparison of PCR cycles with different PID parameters.**

| | PID Parameters | PID Tuning Method | Rise Time | Peak | Overshoot & Undershoot |
|---|---|---|---|---|---|
| **Figure 17** | Kp=100, Ki=35, Kd=150 | Trial & Error | 0.774 sec | 1.06 | +2°C & -2°C |
| **Figure 18** | Kp=1.4602, Ki=3.1074, Kd=0 | MATLAB PID Tuner | 8.44 sec | 1.07 | +4°C & -2°C |

Using the same PCR protocol parameters and PID parameters (Kp, Ki and Kd are 100, 35 and 150, respectively) the Peltier element and cartridge heater (12V, 40W) were used to increase the temperature and the following graph was obtained (Figure 19). As seen in the graph, the denaturation temperature (95ºC) was not reached when the cartridge heater was used. It is believed that this condition results from the cartridge heater's delayed transitions between three temperature steps when it is utilized with PID control.

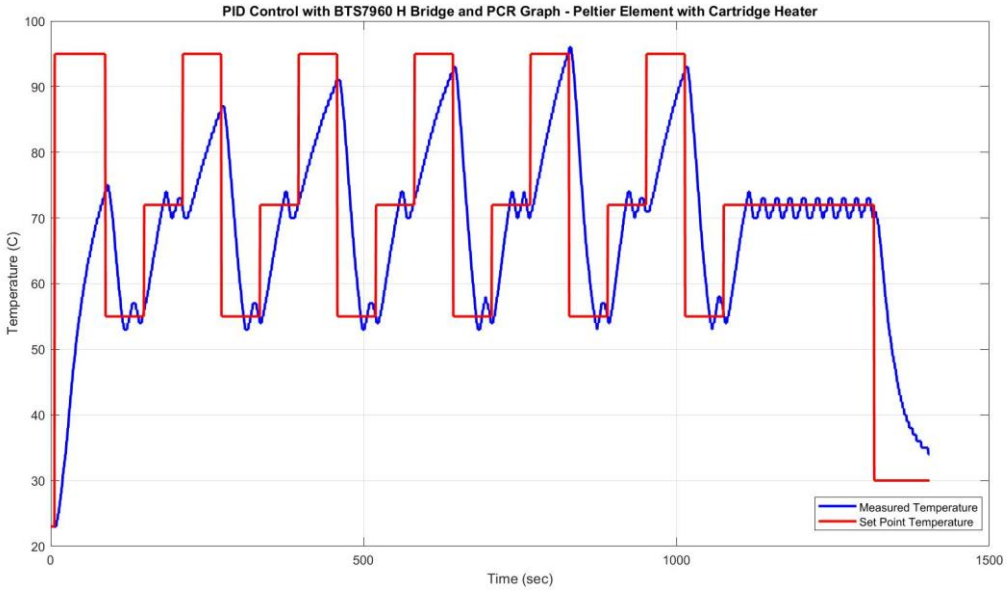


**Figure 19: PCR graph of 5 cycles using Peltier element and cartridge heater (Kp, Ki and Kd are 100, 35 and 150 respectively).**

## 5. Discussion

A thermal cycler was tested and developed. The results demonstrate that a desired temperature can be maintained and controlled by the PID controller. After that, the thermal cycler system that had been developed was tested for five cycles of the entire PCR cycle. The five-cycle PCR with initial denaturation and final extension step, approximately 19-minute PCR procedure is shown in the Table 4 below. While the heating rate from the extension step to the denaturation step was 1.66°C/s; the heating rate from the annealing step to the extension step was 1.55°C/s and the cooling rate was 1.08°C/s. The heating rate of the thermal cycler system is 1.60 °C/s, calculated as the average of 1.55°C/s and

1.66°C/s. The CPU cooling method in our device did not provide a major effect in removing heat from the microchip inside the thermal cycler box.

**Table 4: 5 cycles Thermal Cycler conditions, heating/cooling rates (Calculations were made according to Figure 15)**

| | Temperature Cycler Step Change | Transition Time | Ramp Rate | Temperature Cycler Step |
|---|---|---|---|---|
| ***Start*** | 30°C → 92 °C | 53 sec | 1.17 °C/sec | *Initial Denaturation* |
| ***5 Cycle*** | 92°→ 55°C | 34 sec | 1.08 °C/sec | *Annealing* |
| | 55°C → 72°C | 11 sec | 1.55 °C/sec | *Extension* |
| | 72° → 92°C | 12 sec | 1.66 °C/sec | *Denaturation* |
| ***Total Time*** | **19 min 26 sec** | | | |
| ***Heating rate of the system= (1.55 + 1.66 ) / 2 = 1.60 °C/sec*** | | | | |

The findings of the PCR graph obtained with the PID parameters determined using the PID Tuner Toolbox are summarized in Table 5. The heating rate of this system was slower with 1.135 °C/sec. The cooling rate was same with 1.08 °C/sec. The difference in heating rates can be due to PID parameters. But the fact that the cooling rates are the same suggests that even if the PID parameters are changed, similar results will still be obtained if the materials used are not changed.

**Table 5: 5 cycles Thermal Cycler conditions, heating/cooling rates (Calculations were made according to Figure 18)**

| | Temperature Cycler Step Change | Transition Time | Ramp Rate | Temperature Cycler Step |
|---|---|---|---|---|
| ***Start*** | 30°C → 92 °C | 60 sec | 1.03 °C/sec | *Initial Denaturation* |
| ***5 Cycle*** | 92°→ 55°C | 34 sec | 1.08 °C/sec | *Annealing* |
| | 55°C → 72°C | 12 sec | 1.41 °C/sec | *Extension* |
| | 72° → 92°C | 23 sec | 0.86 °C/sec | *Denaturation* |
| ***Total Time*** | **20 min 19 sec** | | | |
| ***Heating rate of the system= (1.41 + 0.86) / 2 = 1.135 °C/sec*** | | | | |

Because it is difficult to seal the inlet and outlet of the PCR chip and an incomplete seal could cause the sample to evaporate, only the temperature of the heating element Peltier was monitored. Direct measurement of the sample's current temperature was not possible to measure. After making the necessary improvements, a DNA sample will be amplified, and the results will be compared with the result of a conventional thermal cycler.

## 6. Conclusions

For POC testing, a microfluidic device based on the polymerase chain reaction (PCR) technology with a PID temperature controller was created. Designing a PID control algorithm for a PCR thermal cycler involves creating a system that accurately maintains the temperature of PCR samples through precise control loops. When creating this system, the target temperature profile required for the PCR process, including ramping, holding, and cooling stages, is first determined. Information is then collected about the thermal cycler's heating and cooling mechanisms, sensor types, and its limitations in terms of response time or accuracy. The three components of the PID controller need to be understood. It is important to adjust these values according to the characteristics of the system. After the PID parameters are set, the algorithm is created, and a code is generated. Boundaries can be added to the control output to ensure that samples are not overheated or overcooled. This involves limiting the output value or temporarily disabling the integral component when the temperature approaches the limits. After the parameters are set, the control algorithm is tested using simulated thermal cycler. The temperature response is monitored during the ramp, hold, heating and cooling phases. If the response is not satisfactory, it is repeated by adjusting the PID parameters and testing again. PID parameters are improved according to the observed system behavior. The optimization step may include more advanced tuning methods such as manual tuning, Ziegler-Nichols, or trial and error. The effectiveness of the PID control algorithm depends on the accuracy of the temperature sensors, the quality of the heating and cooling mechanisms, and the overall response characteristics of the system.

To conclude we presented an efficient and inexpensive thermal cycler that enables rapid heating of samples that uses a polymer - glass chip and Peltier elements for a microchip-based PCR system. All electrical components soldered on a single PCB. A PCR device was fabricated by combining a centrifugal fan and a CPU fan for cooling, control circuit with a microcontroller to control the Peltier element. Using laser cutting to build a polymer-glass microchip simplified the procedure and significantly decreased the amount of time required to fabricate the microchip. Since the aim of this work is to reach the desired temperatures faster, studies are continuing to make it different from traditional thermal cyclers. The optimization of thermal cycler is continually being improved upon.

## 7. References

1. C. (US) John Girdner Atwood, West Redding, CT (US); Albert Carmelo Mossa, Trumbull, CT (US); Lisa May Goven, Bridgeport, CT (US); Fenton Williams Brookfield, Brookfield, CT (US); Marcel Margulies, Scarsdale, NY (US); Robert P. Ragusa, Newton, CT (US); Richard Lea, “THERMAL CYCLER FOR AUTOMATIC PERFORMANCE OF THE POLYMERASE CHAIN REACTION WITH CLOSE TEMPERATURE CONTROL,” 2004.
2. Y. M. D. Lo and K. C. A. Chan, “Introduction to the polymerase chain reaction.,” *Methods Mol. Biol.*, vol. 336, pp. 1–10, 2006, doi: 10.1385/1-59745-074-x:1.
3. J. A. Carriço, A. J. Sabat, A. W. Friedrich, and M. Ramirez, “Bioinformatics in bacterial molecular epidemiology and public health: Databases, tools and the next-generation sequencing revolution,” *Eurosurveillance*, vol. 18, no. 4, pp. 1–8, 2013, doi: 10.2807/ese.18.04.20382-en.
4. A. G. Jagtar Singh , Niti Birbian, Shweta Sinha, “A critical review on PCR, its types and applications,” *Int. J. Adv. Res. Biol. Sci*, vol. 1, no. 7, pp. 65–80, 2014, [Online]. Available: http://dx.doi.org/10.22192/ijarbs.2021.08.09.001.
5. C. D. Ahrberg, A. Manz, and B. G. Chung, “Polymerase chain reaction in microfluidic devices,” *Lab*

*Chip*, vol. 16, no. 20, pp. 3866–3884, 2016, doi: 10.1039/c6lc00984k.
6. A. Wuethrich and J. P. Quirino, "A decade of microchip electrophoresis for clinical diagnostics – A review of 2008–2017," *Anal. Chim. Acta*, vol. 1045, pp. 42–66, 2019, doi: 10.1016/j.aca.2018.08.009.
7. R. Cuchacovich, "Clinical Applications of the Polymerase Chain Reaction: An Update," *Infect. Dis. Clin. North Am.*, vol. 20, no. 4, pp. 735–758, 2006, doi: 10.1016/j.idc.2006.09.003.
8. M. Joshi and J. D. Deshpande, "Polymerase Chain Reaction: Methods, Principles and Application," *Int. J. Biomed. Res.*, vol. 2, no. 1, 2011, doi: 10.7439/ijbr.v2i1.83.
9. Y. Yang, Y. Chen, H. Tang, N. Zong, and X. Jiang, "Microfluidics for Biomedical Analysis," *Small Methods*, vol. 4, no. 4, pp. 1–30, 2020, doi: 10.1002/smtd.201900451.
10. M. Teymouri *et al.*, "Recent advances and challenges of RT-PCR tests for the diagnosis of COVID-19," *Pathol. Res. Pract.*, vol. 221, no. March, p. 153443, 2021, doi: 10.1016/j.prp.2021.153443.
11. G. R. M. Duarte, C. W. Price, B. H. Augustine, E. Carrilho, and J. P. Landers, "Dynamic solid phase DNA extraction and PCR amplification in polyester-toner based microchip," *Anal. Chem.*, vol. 83, no. 13, pp. 5182–5189, 2011, doi: 10.1021/ac200292m.
12. A. Wuethrich and J. P. Quirino, "A decade of microchip electrophoresis for clinical diagnostics – A review of 2008–2017," *Anal. Chim. Acta*, vol. 1045, pp. 42–66, 2019, doi: 10.1016/j.aca.2018.08.009.
13. A. T. Woolley, D. Hadley, P. Landre, J. Andrew, R. A. Mathies, and M. A. Northrup, "Functional Integration of PCR Amplification and Capillary Electrophoresis in a Microfabricated DNA Analysis Device electrophoresis ( CE ) chips have been successfully coupled," *Anal. Chem.*, vol. 68, no. 23, pp. 4081–4086, 1996.
14. H. Li *et al.*, "Versatile digital polymerase chain reaction chip design, fabrication, and image processing," *Sensors Actuators, B Chem.*, vol. 283, no. November 2018, pp. 677–684, 2019, doi: 10.1016/j.snb.2018.12.072.
15. Y. Zhang and P. Ozdemir, "Microfluidic DNA amplification-A review," *Anal. Chim. Acta*, vol. 638, no. 2, pp. 115–125, 2009, doi: 10.1016/j.aca.2009.02.038.
16. S. Park, Y. Zhang, S. Lin, T. H. Wang, and S. Yang, "Advances in microfluidic PCR for point-of-care infectious disease diagnostics," *Biotechnol. Adv.*, vol. 29, no. 6, pp. 830–839, 2011, doi: 10.1016/j.biotechadv.2011.06.017.
17. N. Y. Lee, "Recent progress in lab-on-a-chip technology and its potential application to clinical diagnoses," *Int. Neurourol. J.*, vol. 17, no. 1, pp. 2–10, 2013, doi: 10.5213/inj.2013.17.1.2.
18. Q. Di HE, D. P. HUANG, G. HUANG, and Z. G. CHEN, "Advance in Research of Microfluidic Polymerase Chain Reaction Chip," *Chinese J. Anal. Chem.*, vol. 44, no. 4, pp. 542–550, 2016, doi: 10.1016/S1872-2040(16)60921-0.
19. N. S. Nise, *Control Sytems Engineering*, Sixth Edit., vol. 517. 2011.
20. K. N. R. V. Sailaja, "PID Controller Tuning using Ziegler-Nichols Method for Temperature control of Thermal Cycler," pp. 1289–1296, 2019, doi: 10.15662/IJAREEIE.2019.0804024.
21. N. R. K. Sailaja Vangimalla, Ramesh Datla, Lakshmi Prasad M, "DESIGN AND DEVELOPMENT OF THERMAL CYCLER (PCR INSTRUMENT) FOR DNA ANALYSIS," *Int. J. Eng. Sci. Res. Technol.*, vol. 8, no. 5, 2019.
22. M. D. Thakor, S. K. Hadia, and A. Kumar, "Precise temperature control through Thermoelectric Cooler with PID controller," *2015 Int. Conf. Commun. Signal Process. ICCSP 2015*, no. June, pp.

1118–1122, 2015, doi: 10.1109/ICCSP.2015.7322677.
23. K. H. Ang, G. Chong, and Y. Li, "PID control system analysis, design, and technology," *IEEE Trans. Control Syst. Technol.*, vol. 13, no. 4, pp. 559–576, 2005, doi: 10.1109/TCST.2005.847331.
24. K. J. Åström and T. Hägglund, "The future of PID control," *Control Eng. Pract.*, vol. 9, no. 11, pp. 1163–1175, 2001, doi: 10.1016/S0967-0661(01)00062-4.
25. O. A. Somefun, K. Akingbade, and F. Dahunsi, "The dilemma of PID tuning," *Annu. Rev. Control*, vol. 52, no. May, pp. 65–74, 2021, doi: 10.1016/j.arcontrol.2021.05.002.
26. B. Copeland, "The Design of PID Controllers using Ziegler Nichols Tuning," *Retrieved, March*, no. March, pp. 1–4, 2008, [Online]. Available: http://educypedia.karadimov.info/library/Ziegler_Nichols.pdf.
27. S. B. Joseph, E. G. Dada, A. Abidemi, D. O. Oyewola, and B. M. Khammas, "Metaheuristic algorithms for PID controller parameters tuning: review, approaches and open problems," *Heliyon*, vol. 8, no. 5, p. e09399, 2022, doi: 10.1016/j.heliyon.2022.e09399.
28. H. I. Jaafar, S. Yuslinda, M. Shahrieel, and M. Aras, "Development of PID Controller for Controlling Desired Level of Coupled Tank System," *Int. J. Innov. Technol. Explor. Eng.*, no. 3, pp. 2278–3075, 2014, [Online]. Available: https://www.researchgate.net/publication/263047616.
29. K. S. Chong, K. B. Gan, and S. Then, "Development of Thermal Cycler Using Proportional-Integral Controller for Polymerase Chain Reaction," *Int. Med. Device Technol. Conf.*, pp. 199–202, 2017.
30. H. E. Kim, A. Schuck, W. Y. Kim, E. K. Jung, Y. H. Hong, and Y. S. Kim, "PID Temperature Control System-Based Microfluidic PCR Chip for Genetic Analysis," *J. Electr. Eng. Technol.*, vol. 17, no. 1, pp. 495–501, 2022, doi: 10.1007/s42835-021-00969-1.
31. L. Li, L. Zhu, Q. Jiang, and G. Liu, "Optimizing of thermal cycler control in microfluidic PCR system," *Appl. Mech. Mater.*, vol. 263–266, no. PART 1, pp. 713–717, 2013, doi: 10.4028/www.scientific.net/AMM.263-266.713.
32. F. Cui *et al.*, "Design and experiment of a PDMS-based PCR chip with reusable heater of optimized electrode," *Microsyst. Technol.*, vol. 23, no. 8, pp. 3069–3079, 2017, doi: 10.1007/s00542-016-3064-3.
33. L. Yao, Y. Jiang, Z. Tan, and W. Wu, "Construction of Very Low-Cost Loop Polymerase Chain Reaction System Based on Proportional-Integral-Derivative Temperature Control Optimization Algorithm and Its Application in Gene Detection," *ACS Omega*, vol. 7, no. 50, pp. 46003–46011, 2022, doi: 10.1021/acsomega.2c02975.
34. C. Kim Soon, N. Anusha Devi, K. Beng Gan, and S.-M. Then, "Design and development of polymerase chain reaction thermal cycler using proportional-integral temperature controller," *Malaysian J. Fundam. Appl. Sci.*, vol. 14, no. 2, pp. 213–218, 2018, doi: 10.11113/mjfas.v14n2.765.
35. V. K. de Oliveira *et al.*, "A low-cost PCR instrument for molecular disease diagnostics based on customized printed circuit board heaters," *Biomed. Microdevices*, vol. 23, no. 2, pp. 1–8, 2021, doi: 10.1007/s10544-021-00563-2.
36. H. Liu *et al.*, "Temperature control algorithm for polymerase chain reaction (PCR) instrumentation based upon improved hybrid fuzzy proportional integral derivative (PID) control," *Instrum. Sci. Technol.*, vol. 51, no. 2, pp. 109–131, 2023, doi: 10.1080/10739149.2022.2105866.
37. T. Pogfai, A. Wisitsoraat, A. Tuantranont, K. Wong-Ek, and S. Mongpraneet, "Low Cost and Portable PCR Thermoelectric Cycle," *Int. J. Appl. Biomed. Eng.*, vol. 1, no. January, pp. 41–45, 2008, [Online]. Available: http://www.nectec.or.th/mems,.